

Spectral Mixing in Nervous Systems: Experimental Evidence and Biologically Plausible Circuits

David KLEINFELD^{1,2,3,*} and Samar B. MEHTA^{2,3}

¹*Dept. of Physics, University of California at San Diego, La Jolla, CA 92093, USA*

²*Neurosciences Graduate Program, University of California at San Diego, La Jolla, CA 92093, USA*

³*Center for Theoretical Biological Physics, University of California at San Diego, La Jolla, CA 92093, USA*

(Received September 14, 2005)

The ability to compute the difference frequency for two periodic signals depends on a nonlinear operation that mixes those signals. Behavioral and psychophysical evidence suggest that such mixing is likely to occur in the vertebrate nervous system as a means to compare rhythmic sensory signals, such as occurs in human audition, and as a means to lock an intrinsic rhythm to a sensory input. Electrophysiological data from electroreceptors in the immobilized electric fish and somatosensory cortex in the anesthetized rat yield direct evidence for such mixing, providing a neurological substrate for the modulation and demodulation of rhythmic neuronal signals. We consider an analytical model of spectral mixing that makes use of the threshold characteristics of neuronal firing and which has features consistent with the experimental observations. This model serves as a guide for constructing circuits that isolate given mixture components. In particular, such circuits can generate nearly pure difference tones from sinusoidal inputs without the use of band-pass filters, in analogy to an image-reject mixer in communications engineering. We speculate that such computations may play a role in coding of sensory input and feedback stabilization of motor output in nervous systems.

§1. Introduction

Oscillations are a hallmark of neuronal activity. When two neuronal oscillators interact through synaptic connections, their respective spike patterns often synchronize or lock with a non-zero phase shift. A dramatic example concerns two cortical neurons that interact via reciprocal inhibitory connections and spike in anti-phase at low firing rate but synchronize at high firing rate.¹⁾ This remarkable shift in behavior was predicted^{2),3)} using the theory of weakly coupled oscillators that was pioneered by Prof. Kuramoto and elucidated so clearly in *Chemical Oscillations, Waves and Turbulence*.⁴⁾ This theory has provided further insight through its application to the dynamics of networks of neurons,⁵⁾ where collective behavior can lead to linear waves of electrical activity in a central olfactory organ^{6)–8)} and rotating waves of electrical activity in visual cortex⁹⁾ and in neocortical slices under epileptic-like states.¹⁰⁾ At a still higher level, the Kuramoto model has been used to study neuronal synchronization in stimulus coding,^{11)–14)} as appears to occur in the processing of multiple stimuli by visual cortex.¹⁵⁾

It is our belief that the application of Prof. Kuramoto's ideas to coupled neurons

^{*}) E-mail: dk@physics.ucsd.edu

represents one of the only two intellectual threads that systematically connects single-cell behavior to network behavior. For weakly coupled neuronal oscillators, this is achieved by the reduction of the full dynamics of each cell to dynamics of a single phase variable that describes the state of a neuron along its limit cycle. The phase variables for different cells are coupled through a sensitivity function, which corresponds to Kuramoto's Z-function, and an interaction function, each of which is described in terms of phase variables so that the output of one cell affects the phase of other cells.⁵⁾ For completeness, the second intellectual thread is the strong coupling of neurons with independent Poisson-spike statistics, either in the limit of large networks¹⁶⁾ or slow synapses;¹⁷⁾ both cases result in a firing rate description that is the key ingredient of attractor neural networks.¹⁸⁾⁻²⁰⁾

Here we turn our attention to a functional consequence of interactions between oscillators in pursuit of the computational role they may play in sensorimotor systems. Motivated by experimental findings, we consider the spectral mixing that can occur between two periodic signals. Mixing provides a mechanism for computing the differences and sums of the frequency content of two signals. This can easily be seen when mixing is accomplished by the multiplication of two sinusoids, $\cos(2\pi f_a t) \times \cos(2\pi f_b t) = \frac{1}{2} \cos[2\pi(f_a - f_b)t] + \frac{1}{2} \cos[2\pi(f_a + f_b)t]$. When combined with a means for isolating the difference term, spectral mixing allows the comparison of even small differences in the frequency content between two signals. This phenomenon is commonly witnessed in audition, where human subjects are sensitive to the beat, or difference, frequency between two simultaneous pure tones.²¹⁾ The perception persists when the frequencies are presented to different ears, indicating a neural rather than a biomechanical substrate for the mixing. Similar computations may be performed in various ethological tasks, including: (i) Electroreception, where animals sense the difference in frequency between their own rhythmic electrical discharge and that of a neighboring fish;^{22),23)} (ii) Echolocation, where the relative speed of flight between a bat and its prey is encoded in the difference in frequency between outgoing and reflected acoustic waves;²⁴⁾ and (iii) Pitch determination, where animals recognize the fundamental frequency of a sound based on a harmonic stack, even when the stack is missing the fundamental.²⁵⁾

If we extend the example to the case in which the two sinusoids are at the same frequency but have a phase difference, we obtain, $\cos(2\pi ft) \times \cos(2\pi ft - \phi) = \frac{1}{2} \cos(\phi) + \frac{1}{2} \cos(4\pi ft - \phi)$. Here, isolating the DC term allows measurement of the relative phase between two signals. Such a function can also be relevant for sensory processing, as in (i) Audition, where the phase difference that results from the time it takes for a sound to reach the two ears serves as a measure of source angle;^{26),27)} and (ii) Vibrissa somatosensation in rats, where the relative phase between a rhythmic motor signal and a touch signal may be used to decode the position of an object relative to the head.²⁸⁾

§2. Electrophysiological evidence for spectral mixing

While spectral mixing would appear to be a useful computation in several systems, we only know of three neurophysiological studies that have observed this phe-

nomenon. We first review these experimental findings and use the data as motivation for a minimal model of spectral mixing by neurons. We then raise a conjecture about circuits that make use of phase shifts, rather than filtering, to isolate desired frequency components after the mixing has occurred.

2.1. Human vision

An experiment by Regan and Regan²⁹⁾ recorded electroencephalograms (EEGs) across visual cortical areas in human subjects as they attended to two superimposed, modulated visual gratings. An analysis of the EEG signals showed that the spectrum contained a term at a frequency of $2f_1 + 2f_2$, where f_1 and f_2 were the temporal modulation frequencies of the two gratings and the factor of 2 is due to the presence of both light-to-dark and dark-to-light transitions.

2.2. Fish electroreception

The sense organ of the paddlefish *Polyodon Spathula*, a species of electric fish, consists of electroreceptors that cover the animal's rostrum, a flat structure that projects from the head (Fig. 1(a)). Neiman and Russell³⁰⁾ demonstrate that this electroreceptor system contains two distinct oscillators. One oscillator exists within a cluster of canals in the epithelia of the sensor and produces oscillations in the range of 10 to 30 Hz. The second oscillator arises from the axon terminals and produces an oscillation in the range of 30 to 70 Hz.

The authors made extracellular recordings from the anterior lateral line nerve (ALLn) (Fig. 1(a)), reporting spiking from a single sensory cell. Their recordings contained rhythmic contributions from both the epithelium, with frequency f_e , and from the afferents, with frequency f_a (Fig. 1(b)). Critically, the authors found mixture terms at frequencies $f_a + f_e$, $f_a - f_e$, and $2f_a - f_e$. Introduction of a sinusoidal external stimulus, with frequency f_s , led to mixing among all three oscillators (Fig. 1(c)). The authors note that this behavior is consistent with mixing of the oscillators, although they prefer an explanation based on synaptic modulation of one oscillator by the other.

2.3. Rat somatosensation

The somatosensory cortex in rat has a prominent region, known as the vibrissa primary somatosensory (S1) cortex, that is devoted to the processing of tactile stimuli from the animal's large facial whiskers, or vibrissae (Fig. 2(a)). Rats move their vibrissae in 5 to 15 Hz exploratory movements and such moving sensors pose a sensory challenge: the spatial meaning of a contact event depends on its phase relative to the oscillating vibrissa position. A plausible model³²⁾ for this problem approximates the position and touch signals as sinusoids, i.e., Motion $\propto 1 + \cos(2\pi f_{motion}t - \phi_{motion})$, where ϕ_{motion} is the preferred phase of a given neuron³¹⁾ and Contact $\propto 1 + \cos[2\pi f_{motion}(t - t_{contact})] + \text{higher-order terms,}^*$ where $t_{contact}$ is the time of contact. Spectral mixing of these two signals leads to an output that contains the phase difference term $\cos(2\pi f_{motion}t_{contact} - \phi_{motion})$, as

*) Higher order terms are needed here to enforce causality, as a periodic touch signal cannot be symmetric about $t_{contact}$.

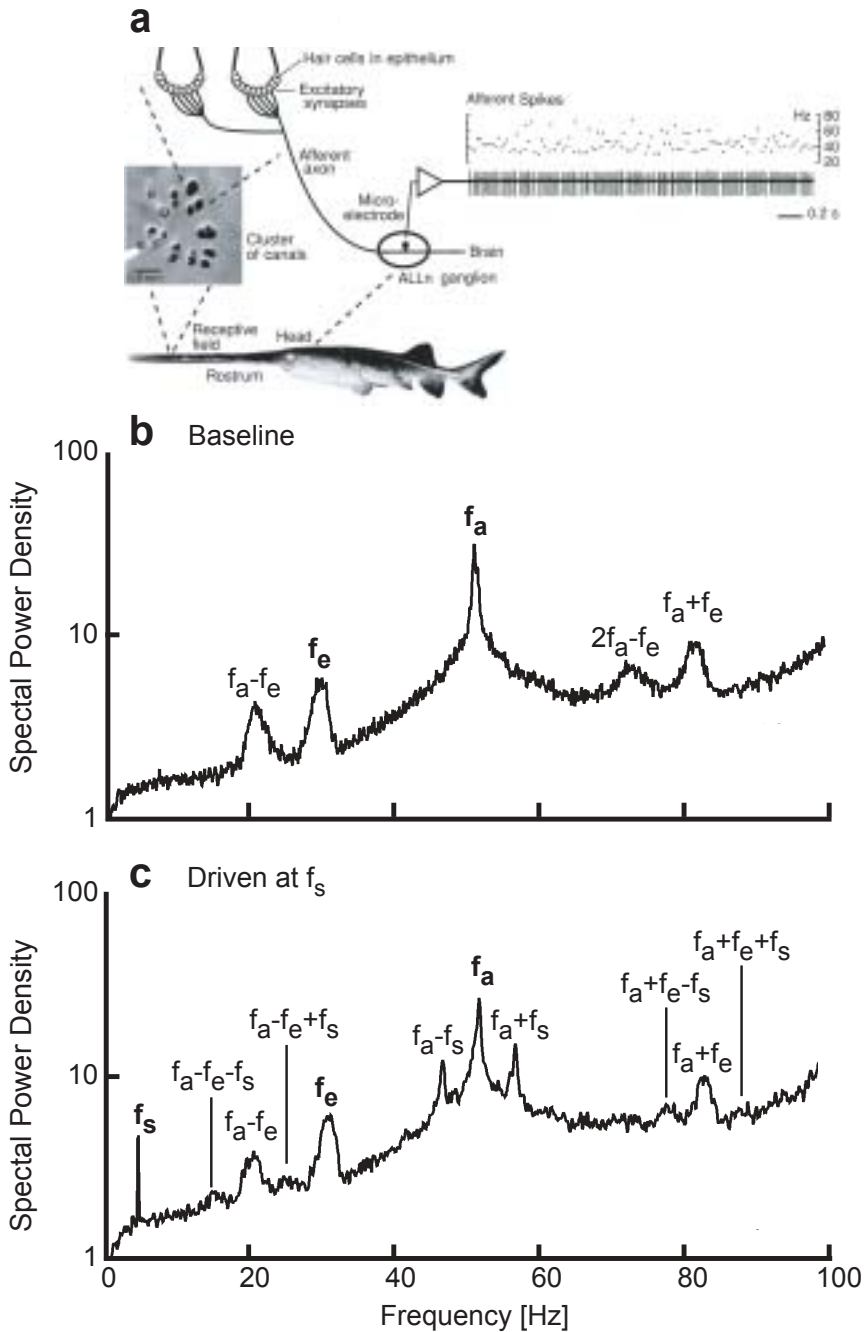


Fig. 1. Mixing in the anterior lateral line afferents in the paddlefish. (a) Diagram of the electroreceptor. Recordings are made from afferents in the afferent lateral line nerve (ALLn) ganglion. The example time series shows an extracellular recording and the corresponding instantaneous frequency. (b) The spectral power of the ALLn signal in the absence of stimulation. Note contributions of the afferent and epithelial oscillators, with frequencies f_a and f_e respectively, as well as the mixture terms. (c) The spectral power during stimulation of the epithelium at frequency f_s . Panels adapted from Ref. 30).

discussed in the introduction above. If this term is isolated, the resulting spike rate will be highest when contact occurs at particular phase relative to vibrissa motion; preliminary data provides evidence for such a signal in behaving animals.³³⁾

an external stimulus with frequency f_s was turned on at time zero.

In our laboratory, Ahrens et al.³⁴⁾ studied the underlying computation by introducing two incommensurate frequencies into the cortex of an anesthetized rat. An intrinsic oscillation (centered at frequencies f_i from 2 to 5 Hz) was introduced to cortex through the application of the anesthetic ketamine, and a second oscillation was added using mechanical stimulation of the vibrissae at frequencies f_s in the range 5 to 15 Hz (Fig. 2(b)). The authors observed only intrinsic oscillations in the absence of a mechanical stimulus. During stimulation, however, they found the addition of both the stimulus frequency and the mixture frequencies $f_s \pm f_i$ (Figs. 2(b) and (c)). Higher-order mixture terms, such as $2f_s - f_i$, here likely result from harmonics in the punctate shape of the stimulus rather than from the nonlinearity responsible for mixing. The authors found similar results when the two frequencies were separately applied to the two sides of the head in a procedure reminiscent of binaural mixing in audition, rather than using the anesthesia induced oscillations.

§3. Threshold model for mixing

We now turn our attention to a phenomenological model of the experimental findings. The results for the paddlefish electroreceptive organ and the rat vibrissa S1 cortex have a number of common features: (i) The “input” frequencies, e.g., f_s and f_i in Fig. 2, are present in the output; (ii) Primary mixing terms, e.g., $f_a + f_e$ and $f_a - f_e$ in Fig. 2, are present in roughly equal proportion; and (iii) Higher-order terms, such as harmonics of the inputs, are present at the output. Any of a number of cellular nonlinearities^{35),36)} may account for these observations. We focus on the consequences of the threshold firing properties of a neuron and consider a simple but analytically tractable model.

We describe a rhythmic post-synaptic input to a neuron as

$$x(t) = \cos(2\pi f_a t + \phi_a) + \rho \cos(2\pi f_b t + \phi_b), \quad (1)$$

with $0 < \rho \leq 1$, and consider the threshold relation given by

$$y(t) = [x(t) - \theta_0]_+, \quad (2)$$

where θ_0 is the value of the threshold and $[f(t)]_+$ is the Heaviside function, i.e., $y(t) = 0$ when $x(t) < \theta_0$ and $y(t) = 1$ when $x(t) \geq \theta_0$. The output can be expressed in terms of closed integrals³⁴⁾ to yield

$$y(t) = \frac{1}{2\pi i} \sum_{n=-\infty}^{\infty} \sum_{m=-\infty}^{\infty} I_{n,m}(\theta_0, \rho) e^{i[n(\phi_a + \pi/2) + m(\phi_b + \pi/2)]} e^{2\pi i(nf_a + mf_b)t}, \quad (3)$$

for integer mixture coefficients m and n . The first factor,

$$I_{n,m}(\theta_0, \rho) \triangleq \lim_{\epsilon \rightarrow 0} \int_{-\infty}^{\infty} \frac{d\Omega}{\Omega - i\epsilon} e^{-i\theta_0\Omega} J_n(\Omega) J_m(\rho\Omega), \quad (4)$$

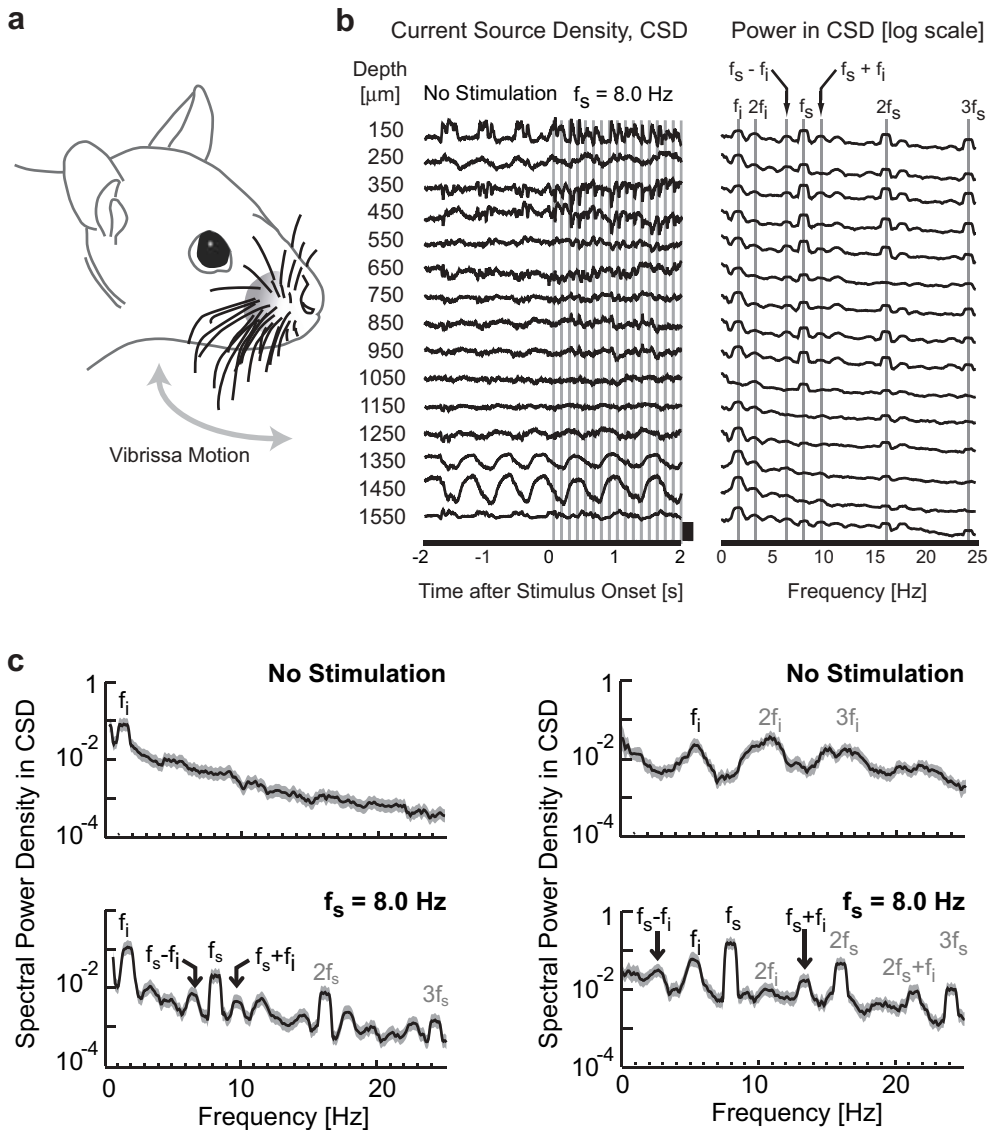


Fig. 2. Mixing in the vibrissa primary sensory cortex from rat. (a) Cartoon showing the vibrissae and their axis of motion. (b) Example recordings from different depths in vibrissa S1 cortex. The data on the left are time series of the the current source density (CSD), which is the discrete second derivative of the measured voltage and approximates the divergence of current flow (scale bar 10 mV/mm²). An external stimulus with frequency f_s was turned on at time zero. The panel on the right shows the spectral power for the same depths during stimulation. Note the presence of mixture frequencies $f_s \pm f_i$. (c) The spectral power before (top panels) and after (bottom panels) stimulation at a depth of 450 μm . Higher order mixture terms and harmonics due to the non-sinusoidal nature of both intrinsic and stimulus-induced oscillations give rise to the peaks indicated by gray text. Gray bands correspond to 95% confidence intervals. Panels (b) and (c) adapted from Ref. 34).

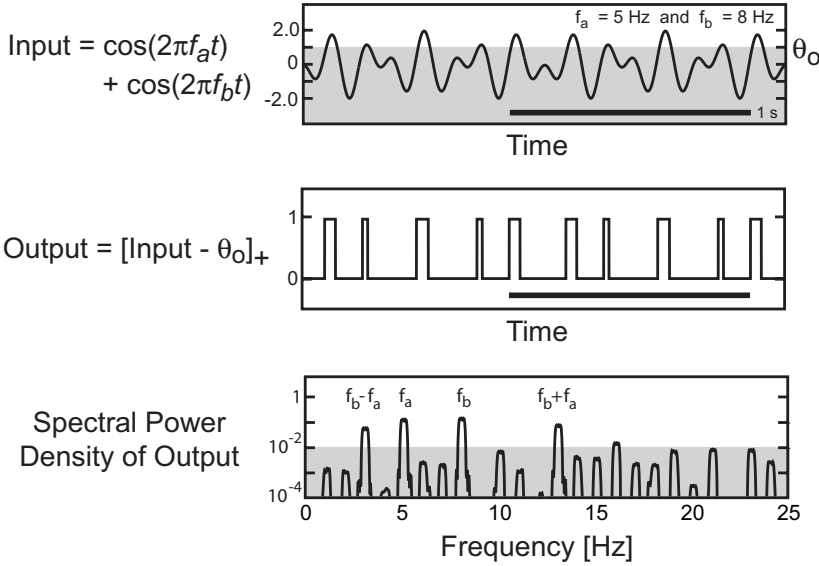


Fig. 3. Threshold mixer example. The top panel shows the summed input signals and threshold level θ_0 (gray band). The middle panel shows the result of applying the transformation in Eq. 2 to the input. The bottom panel shows the power spectrum computed from a 10 sec output time series. The gray band here indicates approximately one decade below the power of the fundamentals. Parameters were set to $\rho = 1.0$, $f_a = 5$ Hz, $f_b = 8$ Hz, and $\theta_0 = 0.8$. Panels adapted from Ref. 34).

is an integral over Bessel functions that sets the magnitude of each mixture term, and must, in general, be evaluated numerically. The second factor sets the phase of each term in the sum and the final factor represents a sinusoid at one of the mixing frequencies, $|mf_a \pm nf_b|$. We recall that $J_k(\Omega) = (-1)^k J_{-k}(\Omega)$, so that $I_{n,-m}(\theta_0, \rho) = (-1)^m I_{n,m}(\theta_0, \rho)$ and sum and difference terms of the same order have equivalent magnitudes. The spectral representation for the output of the model is given by

$$\begin{aligned} \tilde{y}(f) &\triangleq \int_{-\infty}^{\infty} e^{2\pi i f t} y(t) dt \\ &= \frac{1}{2\pi i} \sum_{n=-\infty}^{\infty} \sum_{m=-\infty}^{\infty} I_{n,m}(\theta_0, \rho) e^{i[n(\phi_a + \pi/2) + m(\phi_b + \pi/2)]} \delta[f - (nf_a + mf_b)], \end{aligned} \quad (5)$$

where $\delta()$ is the Dirac delta function. We see that $\tilde{y}(f)$ has contributions at all possible mixture frequencies. Numerical calculations show that the magnitude of the $I_{1,\pm 1}(\theta_0, \rho)$ terms, and thus the spectral power in the sum and difference modes, is maximized for $\rho = 1.0$ and $\theta_0 = 0.8$.³⁴⁾ An example of the threshold process and resulting power spectrum is shown for these parameters in Fig. 3.

§4. Multi-stage mixers for isolation of spectral components

The output from the threshold-based mixer contains components at the fundamental frequencies, their harmonics, the sum and difference mixture terms, and higher order mixtures. In principle, a band-pass filter could be used to isolate one of these components. This method is limited, however, as the frequencies of neighboring components may be close to each other in value. An alternative method uses interference effects in a manner analogous to the structure of image-reject mixers in communications engineering.³⁷⁾ The inputs to two or more threshold units are phase-shifted and the outputs summed, in such a way that undesired components cancel. This requires that we introduce additional circuit elements that can shift the phase of each of the two inputs. Although a simple delay line could accomplish this for a fixed frequency, we describe next a solution that works over a range of frequencies.

4.1. Phase shifters

We first consider the special but useful cases of shifts of $\phi = \pi$ radians, $\phi = \pi/2$ radians, and $\phi = -\pi/2$ radians.

Phase shifting by a factor of π radians can be accomplished with a fast inhibitory synapse, so that the corresponding post-synaptic input to the threshold unit is negative going rather than positive going (Fig. 4(a)). Then,

$$\phi_{output} = \phi_{input} + \pi, \quad (6)$$

corresponding to inversion of the signal.

A phase shift of $\pi/2$ radians arises naturally in the neuronal implementation of a phase-locked loop (PLL),^{38)–41)} which is a feedback circuit that adjusts the frequency of a local oscillator to match that of an input signal.⁴²⁾ A generic analog PLL consists of three components. First, a mixer multiplies the input oscillator by the output of a local oscillator. Second, a low-pass filter $K(t)$ isolates the error term, $\epsilon(t)$, where

$$\epsilon(t) \propto \int_{-\infty}^t d\tau K(t - \tau) \cos(2\pi f_{input}\tau + \phi_{input}) \cos(2\pi f_{local}\tau + \phi_{local} - \pi/2).$$

Third, the frequency of the local oscillator is shifted so that $f_{local} = f_0 + g\epsilon(t)$, where f_0 is a center frequency and g is a gain factor. When the PLL locks, $f_{local} \approx f_{input}$ and $\epsilon(t) \propto \sin(\phi_{input} - \phi_{local})$.

Self-consistency requires that the measured phase, ϕ_{out} , at the output of a locked PLL is of the approximate form

$$\phi_{out} \approx \phi_{input} + \frac{\pi}{2} + \sin^{-1} \left(\frac{f_{input} - f_0}{G} \right), \quad (7)$$

where the constant G is proportional to the gain factor g .^{*)} The local oscillator and the input will tend to be $\pi/2$ radians out of phase when either the gain g , and thus

^{*)} The factor of $\pi/2$ is commonly implicit in textbook formulas, as the local oscillator is described by a sine function while the external input is given as a cosine. This factor was inadvertently dropped in Eq. (10) of Ref. 41).

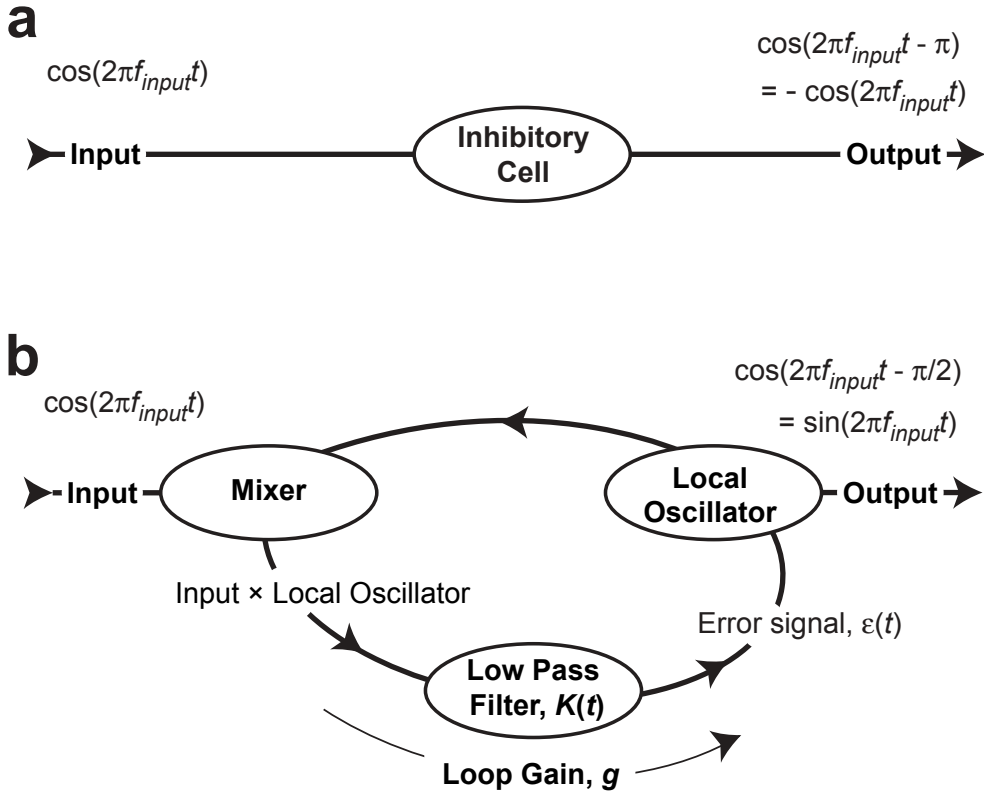


Fig. 4. Phase shifter circuits. (a) Shift of π radians via an inhibitory interneuron that functions as an inverting but otherwise linear input-output device. (b) Shift of $\pi/2$ radians with a phase-lock loop that consists of 3 neurons: one operating as a mixer, one acting as a low-pass filter, and an oscillator whose frequency is a monotonically increasing function of its input.

the constant G , is large or the input frequency f_{input} is close to the intrinsic frequency f_0 . Intuitively, the shift of $\pi/2$ radians occurs because for a PLL at steady-state, the product of the input sinusoid and the local oscillator must average to zero when the PLL is at steady-state.

With the above results, we note that a phase shift of $-\pi/2$ is readily achieved by following a phase shift of $\pi/2$ (Eq. (7)) with an inversion (Eq. (6)).

4.2. A circuit to isolate the difference frequency

We use a mixer in combination with phase shifters of π and $\pm\pi/2$ radians to construct outputs that differ only in the phase term $\exp\{i[n(\phi_a + \pi/2) + m(\phi_b + \pi/2)]\}$ from Eqs. (3) and (5). The phase shifts are chosen so that summation of the outputs leads to a cancellation of the input sinusoids, their harmonics, and the sum frequency, as in an image-reject mixer.³⁷⁾

As a step toward the design of the difference circuit, we first consider the cancellation of the fundamental frequencies. We start with two inputs of equal amplitude, labeled a and b , and two threshold units, labeled 1 and 2. We then define

$\cos(2\pi f_a + \phi_{a,1})$, as the input a , phase-shifted by $\phi_{a,1}$, to threshold unit 1; analogous expressions apply for all combinations of inputs and outputs. From the phase term above, we find that the output at each input frequency, corresponding to mixture terms ($n = 1, m = 0$) and ($n = 0, m = 1$), is simply phase-shifted by $\pi/2$ relative to the input. We thus choose, e.g.,

$$\begin{aligned}\phi_{a,1} &= 0 & \text{and} & & \phi_{b,1} &= \pi, \\ \phi_{a,2} &= \pi & \text{and} & & \phi_{b,2} &= 0,\end{aligned}$$

with the result that the output terms for the fundamentals cancel when summed. The summed output, $Y(t) = y_1(t) + y_2(t)$, is given by

$$\begin{aligned}Y(t) &= \frac{i}{\pi} I_{0,0}(\theta_0, 1) - \frac{i}{\pi} \{ \cos[2\pi(f_a + f_b)t] + \cos[2\pi(f_a - f_b)t] \} I_{1,1}(\theta_0, 1) \\ &+ O(|n| + |m| > 2).\end{aligned}\tag{8}$$

Apart from the constant term, the output is similar to that for multiplication.

We now move to the case of maintaining only the primary difference term. In principle, this can be done with three mixers and phase shifts of $\phi = 0, +2\pi/3$ and $-2\pi/3$ radians, but such shifts are difficult to generate. We consider an alternative scheme with four threshold units, where the phase of the input to each unit is given by

$$\begin{aligned}\phi_{a,1} &= 0 & \text{and} & & \phi_{b,1} &= \pi, \\ \phi_{a,2} &= \pi & \text{and} & & \phi_{b,2} &= 0, \\ \phi_{a,3} &= +\pi/2 & \text{and} & & \phi_{b,3} &= -\pi/2, \\ \phi_{a,4} &= -\pi/2 & \text{and} & & \phi_{b,4} &= +\pi/2.\end{aligned}$$

The summed output, $Y(t) = y_1(t) + y_2(t) + y_3(t) + y_4(t)$, is then

$$Y(t) = \frac{2i}{\pi} I_{0,0}(\theta_0, 1) + \frac{4i}{\pi} \cos[2\pi(f_a - f_b)t] I_{1,1}(\theta_0, 1) + O(|n| + |m| > 2).\tag{9}$$

The difference circuit is illustrated schematically in Fig. 5(a), together with the calculated results for the spectral power density for the choices $f_a = 8$ Hz and $f_b = 5$ Hz (Fig. 5(b)), demonstrating that the fundamentals are almost entirely suppressed.

We note that a straightforward modification of this circuit will preserve the sum rather than the difference terms.

§5. Discussion

Spectral mixing is an integral aspect of electronic communication, as it provides a means to detect and isolate specific frequency components. Certain designs, such as double-balanced mixers and image-reject mixers, exploit the summation of phase-shifted replicas to cancel out designated terms, much as interference effects are used to direct radio signals from antenna arrays and to produce patterned illumination in optics. It is of interest that despite the central role played by oscillators in nervous systems, analogies to these spectral mixers have not been identified *in vivo*.

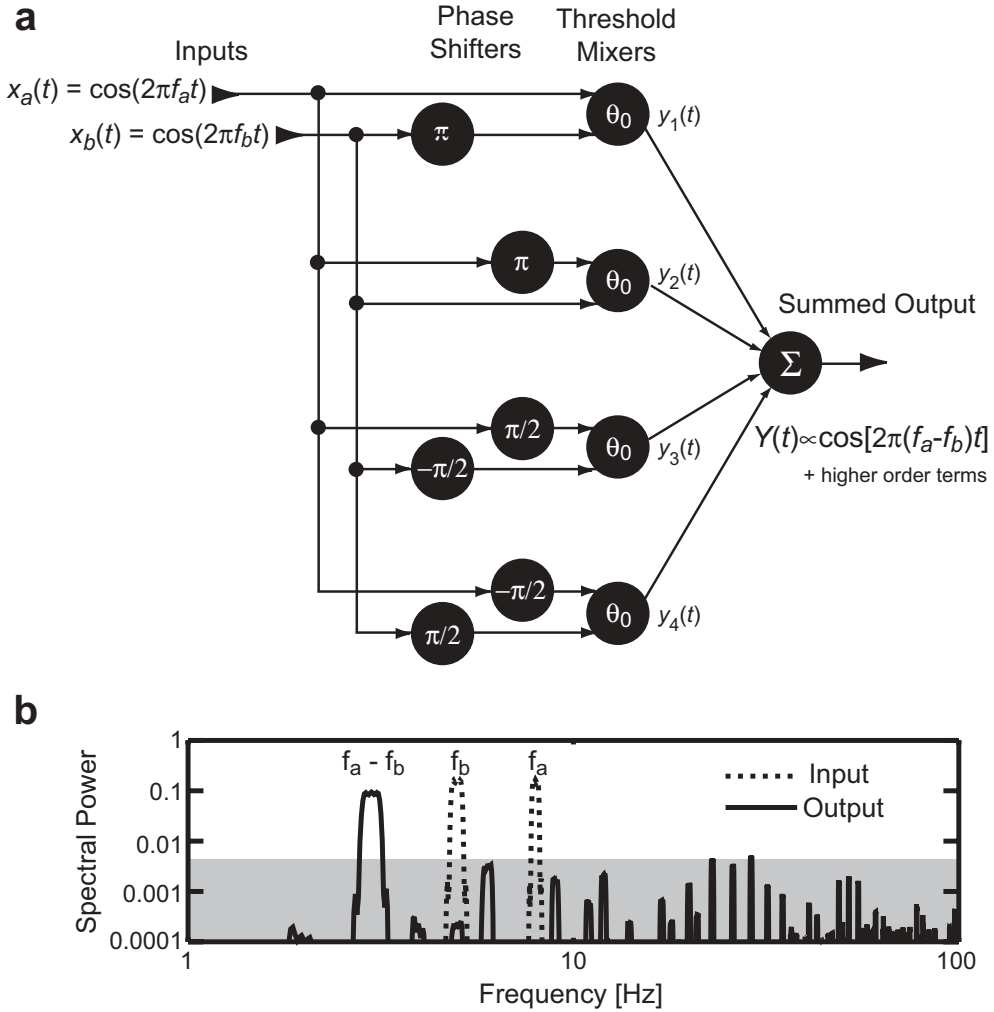


Fig. 5. Neuronal image-reject mixer circuit. (a) Schematic of the circuit, which consists of phase-shifters of π , $\pi/2$ and $-\pi/2$ radians (Eqs. (6) and (7)), threshold units that act as mixers (Eq. (5)), and a linear summation element. (b) Spectral analysis of the output of the mixer circuit in Eq. (9) for input sinusoids with $f_a = 8$ Hz and $f_b = 5$ Hz, and where $\theta_0 = 0$. The gray band indicates the power in the largest of the higher-order components.

Given the presence of mixing terms in the experiments cited above, it is tempting to conjecture that spectral mixing plays a role in neuronal computations. We thus attempted here to demonstrate an implementation that is biologically plausible, although experimental evidence for a neuronal implementation of a PLL is admittedly weak.

As a technical issue, one weakness of our scheme is the need for constant phase shifts over a broad range of frequencies. We choose to use phase-locked loops, a common element in communication and control circuits,⁴²⁾ but even these engineering implementations have limitations. Locking will not occur if the loop gain is too small, while a PLL will lock to a harmonic if the loop gain is too large. In engineer-

ing applications, the latter issue typically limits the useful frequency range of a PLL in the absence of additional circuitry. For example, initial locking may require that the intrinsic frequency be swept, starting near $f_0 = 0$, so that locking occurs at the fundamental.

Our focus has been on mixing to form the difference and sum terms $f_a \pm f_b$, which are prevalent in the experimental data summarized here. Other mixing terms are also of potential interest, however, such as a $2f_a - f_b$ term that arises in psychoacoustics.⁴³⁾ Although these terms can be generated by spectral mixing, alternative formulations are possible. For example, mixing terms can also arise if one oscillator directly provides synaptic modulation to another,³⁰⁾ rather than two oscillators summing in a third threshold unit. As an example of such a system, and as a closing nod to the Kuramoto model, we consider a system of two phase oscillators with unidirectional coupling:

$$\frac{d\phi}{dt} = 2\pi[f_0 + K \sin(2\pi f_d t - \phi)], \quad (10)$$

where $\phi(t)$ is the phase of the driven oscillator, f_0 is its intrinsic frequency, f_d is the frequency of the driving oscillator, and K is the coupling strength.

The dimensionless ratio $K/|f_0 - f_d|$ determines the behavior of this system. If this ratio is smaller than one, the driven oscillator will not entrain to the drive and instead undergoes phase walk-through.⁴⁴⁾ In this case, we obtain an explicit solution for $\phi(t)$ as

$$\phi(t) = 2\pi f_d t - 4\pi \tan^{-1} \left\{ \frac{K + \sqrt{(f_0 - f_d)^2 - K^2} \tan \left[\frac{1}{2} \sqrt{(f_0 - f_d)^2 - K^2} (t + C) \right]}{f_0 - f_d} \right\}, \quad (11)$$

where C is a constant. A sinusoidal oscillator with this phase can be shown to contain spectral components at frequencies given by $f_d \pm m\sqrt{(f_0 - f_d)^2 - K^2}$, for integer m . In the limit that $K \ll |f_0 - f_d|$, the driven oscillator has power at frequencies $\{f_d, f_0, 2f_0 - f_d, f_0 - 2f_d, \dots\}$, demonstrating another plausible route to generating nonlinear mixing terms from the interaction of neuronal oscillators.

Acknowledgements

We thank the NIMH (DK), the NCCR (DK), and the HHMI (SBM) for support.

References

- 1) J. R. Gibson, M. Beierlein and B. W. Connors, *J. Neurophys.* **93** (2005), 467.
- 2) D. Hansel, G. Mato and C. Meunier, *Europhys. Lett.* **23** (1993), 367.
- 3) C. von der Vreeswijk, L. F. Abbott and G. B. Ermentrout, *J. Comput. Neurosci.* **4** (1994), 313.
- 4) Y. Kuramoto, *Chemical Oscillations, Waves and Turbulence* (Springer Verlag, New York, 1984).
- 5) G. B. Ermentrout and D. Kleinfeld, *Neuron* **29** (2001), 1.
- 6) K. R. Delaney, A. Gelperin, M. S. Fee, J. A. Flores, R. Gervais, D. W. Tank and D. Kleinfeld, *Proc. Natl. Acad. Sci.* **91** (1994), 669.

- 7) G. B. Ermentrout, J. Flores and A. Gelperin, *J. Neurophys.* **79** (1998), 2677.
- 8) R. W. Friedrich, C. J. Habermann and G. Laurent, *Nature Neurosci.* **7** (2004), 862.
- 9) J. C. Pechtl, L. B. Cohen, P. P. Mitra, B. Pesaran and D. Kleinfeld, *Proc. Natl. Acad. Sci.* **94** (1997), 7621.
- 10) X. Huang, W. C. Troy, Q. Yang, H. Ma, C. R. Laing, S. J. Schiff and J. Y. Wu, *J. Neurosci.* **24** (2004), 9897.
- 11) H. G. Schuster and P. Wagner, *Biol. Cybernetics* **64** (1990), 77.
- 12) H. G. Schuster and P. Wagner, *Biol. Cybernetics* **64** (1990), 83.
- 13) H. Sompolinsky, D. Golomb and D. Kleinfeld, *Phys. Rev. A* **43** (1991), 6990.
- 14) E. R. Grannan, D. Kleinfeld and H. Sompolinsky, *Neural Computation* **5** (1993), 550.
- 15) C. M. Gray, P. Konig, A. K. Engel and W. Singer, *Nature* **338** (1989), 334.
- 16) O. Shriki, D. Hansel and H. Sompolinsky, *Neural Computation* **15** (2003), 1809.
- 17) B. Ermentrout, *Neural Computation* **6** (1994), 679.
- 18) H. R. Wilson and J. D. Cowan, *Biophys. J.* **12** (1973), 1.
- 19) J. J. Hopfield, *Proc. Natl. Acad. Sci.* **79** (1982), 2554.
- 20) D. J. Amit, *Modeling Brain Function: The World of Attractor Neural Networks* (Cambridge University Press, Cambridge, 1989).
- 21) G. Oster, *Scientific American* **229** (1973), 94.
- 22) T. H. Bullock and W. Heiligenberg, *Electroreception* (Wiley, New York, 1987).
- 23) W. Heiligenberg and G. Rose, *J. Neurosci.* **5** (1985), 515.
- 24) N. Suga, Y. Zhang and J. Yan, *J. Neurophys.* **77** (1997), 2098.
- 25) D. J. Levitin and S. E. Rogers, *Trends in Cognitive Science* **9** (2005), 26.
- 26) J. L. Pena and M. Konishi, *Science* **292** (2001), 249.
- 27) J. L. Pena and M. Konishi, *J. Neurosci.* **24** (2004), 8907.
- 28) E. Ahissar and D. Kleinfeld, *Cerebral Cortex* **13** (2003), 53.
- 29) D. Regan and M. P. Regan, *Vision Reserach* **27** (1987), 2181.
- 30) A. B. Neiman and D. F. Russell, *J. Neurophys.* **92** (2004), 492.
- 31) M. S. Fee, P. P. Mitra and D. Kleinfeld, *J. Neurophys.* **78** (1997), 1144.
- 32) S. B. Mehta and D. Kleinfeld, *Neuron* **41** (2004), 181.
- 33) J. Curtis and D. Kleinfeld, in *Barrels XVIII* (2005).
- 34) K. F. Ahrens, H. Levine, H. Suhl and D. Kleinfeld, *Proc. Natl. Acad. Sci.* **99** (2002), 15176.
- 35) C. Koch and T. Poggio, in *Single Neuron Computation*, ed. T. McKenna, J. Davis and S. E. Zornetzer (Wiley, New York, 1992).
- 36) F. Gabbiani, H. G. Krapp, N. Hatsopoulos, C. H. Mo, C. Koch and G. Laurent, *J. Physiology (Paris)* **98** (2004), 19.
- 37) P. Horowitz and W. Hill, *The Art of Electronics* (Cambridge University Press, Cambridge, 1989).
- 38) E. Ahissar and E. Vaadia, *Proc. Natl. Acad. Sci.* **87** (1990), 8935.
- 39) E. Ahissar, *Neural Computation* **10** (1998), 597.
- 40) F. C. Hoppensteadt, *An Introduction to the Mathematics of Neurons. Modeling in the Frequency Domain* (Cambridge University Press, Cambridge, 1997).
- 41) D. Kleinfeld, R. N. S. Sachdev, L. M. Merchant, M. R. Jarvis and F. F. Ebner, *Neuron* **34** (2002), 1021.
- 42) R. E. Best, *Phase-Locked Loops: Theory, Design, and Applications* (McGraw-Hill, New York, 1984).
- 43) W. M. Hartmann, *Signals, Sound, and Sensation* (American Institute of Physics, Woodbury, 1997).
- 44) G. B. Ermentrout and J. Rinzel, *Am. J. Physiol.* **246** (1984), R102.